Effect of CO_2, H_2O and SO_2 in the ceria-catalyzed combustion of soot under simulated diesel exhaust conditions.

Ana M. Hernández-Giménez, Dolores Lozano-Castelló, Agustín Bueno-López*.

Department of Inorganic Chemistry. University of Alicante, Ap.99, E-03080 Alicante (Spain).

*Corresponding author: email: agus@ua.es;Tel. +34 600948665; Fax. +34 965903454

Abstract

The effect of CO_2, H_2O and SO_2 in the $Ce_{0.73}Zr_{0.27}O_2$ and $Ce_{0.64}Zr_{0.27}Nd_{0.09}O_2$ catalyzed combustion of soot with NOx + O_2 has been studied. Combustion experiments performed in a fix-bed reactor with soot-catalyst mixtures prepared in loose contact mode showed that CO_2, H_2O and SO_2 lower the activity of both catalysts, and the inhibiting effect follows the trend SO_2 > H_2O > CO_2. Regardless the gas mixture composition, the catalytic activity for soot combustion of $Ce_{0.64}Zr_{0.27}Nd_{0.09}O_2$ is equal or higher to that of $Ce_{0.73}Zr_{0.27}O_2$ because Nd^{3+} doping seems to promote the participation of the active oxygen mechanism together with the NO_2-assisted mechanism in the catalytic combustion of soot. The maximum soot combustion rate achieved during a $Ce_{0.64}Zr_{0.27}Nd_{0.09}O_2$-catalyzed reaction in NOx/O_2/CO_2/H_2O/N_2 is about three times higher than that of the uncatalyzed combustion, and this catalyst also improves the CO_2 selectivity.

In situ DRIFTS experiments showed that CO_2, H_2O and SO_2 compete with NOx for the adsorption sites on the catalysts' surface. CO_2 partially impedes the catalytic oxidation of NO to NO_2, affecting much more to the Nd^{3+}-containing catalyst; however, the contribution of the active oxygen mechanism seems to remain relevant in this case. H_2O also hinders the catalytic oxidation of NO to NO_2 on both catalysts, and therefore the catalytic combustion of soot, because delays the formation of nitrogen reaction intermediates on the catalysts' surface and favors the formation of more stable nitrogen surface species than in a H_2O-free gas stream. For both catalysts, SO_2 chemisorption (with sulfate formation) is even able to remove nitrogen surface groups previously formed by NOx chemisorption, which significantly inhibits the catalytic oxidation of NO to NO_2 and the catalytic combustion of soot.

Keywords: Diesel soot; soot combustion; ceria-zirconia catalyst; neodymium-ceria catalyst; nitrogen oxides.

1.- Introduction.

Catalytic combustion of diesel soot is a topic of ongoing research [1-4], and different catalysts have been investigated for this purpose at laboratory scale. These catalysts include formulations with noble metals, alkali metals, alkali earth metals, and transition/internal transition metals that can accomplish redox cycles (V, Mn, Co, Cu, Fe, Ce, Pr, etc) [5].

Platinum catalysts seem the most interesting for practical applications because they combine high activity and stability [6-8], but due to the high price of noble metals, cheaper catalysts are being investigated. Considering the laboratory results obtained by several research groups [4, 5, 9-11], ceria-based catalysts have been proposed as promising substitutes of platinum catalysts. However, extrapolation of laboratory results to real conditions must been done having in mind that, to obtain laboratory results with practical relevance, several aspects must be taken into account.

Attention must be paid to the soot-catalyst contact, and it is usually accepted that “loose contact” mixtures of soot and powder catalysts (soot and catalyst are mixed with a spatula, for instance) simulate the poor contact attained in a real diesel particulate filter.

Thermal stability of catalysts is also a major issue to pay attention to in laboratory studies. Usually, the exhaust temperature in a diesel vehicle is lower than 500 ºC, but hot spots are formed during the regeneration of the diesel particulate filters where the temperature can increase out of control.

The presence of NOx in the gas mixture also plays a key role in the catalytic combustion of soot, and laboratory experiments with practical interest

63 are usually performed with a gas mixture of NO + O_2. NO_2 can be produced in
64 these mixtures, which reacts with soot much faster than NO and O_2.

65 All these aspects have been taken into account in many articles devoted
66 to the study of soot combustion ceria-based catalysts at laboratory [9], but not
67 so attention has been paid to the effect of CO_2, H_2O and SO_2 in the catalytic
68 performance of ceria catalysts, despite these gases are typically present in a
69 diesel exhaust gas.

70 Some authors have reported the poisoning effect of SO_2 on ceria-
71 containing soot combustion catalysts [12-15]. Weng el at. [13] studied the
72 catalytic combustion of soot in NOx + O_2 with Cu-K/CeO_2 catalysts that were
73 previously treated in a 400 ppm SO_2 stream at 400 ºC, and a decrease on the
74 activity was noticed. This deactivation was attributed to potassium sulfate
75 formation, but the effect SO_2 on the ceria behavior was not discussed.

76 The effect of H_2O and SO_2 on the stability of Ba,K/CeO_2 catalysts during
77 diesel soot combustion was also studied [14], and it was concluded that these
78 catalysts had good tolerance to water at low temperatures (e.g., 400 ºC) while
79 high concentrations of SO_2 lead to rapid deactivation. The formation of
80 potassium, barium and cerium sulfates was reported, but the particular effect of
81 H_2O (if any) and SO_2 on the performance of ceria was not analyzed in detail.

82 MnOx-CeO_2 mixed oxides were also tested for the low-temperature
83 oxidation of diesel soot in a O_2 + H_2O + NO + N_2 gas stream, and the effect of
84 SO_2 was also studied [15]. The poisoning effect of SO_2 was also reported in this
85 case, but a detailed analysis of its effect on ceria was not provided apart from
86 the evidences obtained by thermogravimetry about sulfates formation.

The goal of the current study is to analyze the effect of CO_2, H_2O and SO_2 in the ceria-catalyzed combustion of soot in simulated diesel exhaust conditions. Taking into account our previous results [16, 17], and in order to provide practical relevance to the study, two catalysts with composition $Ce_{0.73}Zr_{0.27}O_2$ and $Ce_{0.64}Zr_{0.27}Nd_{0.09}O_2$ have been selected for this study, since they combine a good thermal stability and catalytic activity for soot combustion. As previously concluded, Zr^{4+}-doping is mandatory for a suitable thermal stability of ceria, and Nd^{3+}-doping further improves the activity [17]. Not only a descriptive discussion of the CO_2, H_2O and SO_2 effect on the catalytic soot combustion has been done based on fix-bed reactor experiments, but special attention has been paid to the effect of these gases in the soot combustion mechanism. For this purpose, *in situ* DRIFTS experiments have been carried out.

2.- Experimental.

2.1. Catalysts used.

Details about the preparation and characterization of the $Ce_{0.73}Zr_{0.27}O_2$ and $Ce_{0.64}Zr_{0.27}Nd_{0.09}O_2$ catalysts were previously reported [17]. In brief, the required amounts of $Ce(NO_3)_3{\cdot}6H_2O$ (Sigma Aldrich, 99%), $Nd(NO_3)_3{\cdot}6H_2O$ (Aldrich, 99.9%) and/or $ZrO(NO_3)_2{\cdot}xH_2O$ (Fluka, $x \approx 6$) were dissolved in water and co-precipitation was carried out by dropping an ammonia solution to keep the pH at about 9. After filtering, the precipitate was dried at 110 ºC in air overnight and calcined in air at 800 ºC for 90 min.

Formally, the stoichiometric coefficient of oxygen on $Ce_{0.64}Zr_{0.27}Nd_{0.09}O_2$ should be lower than 2, since the tetravalent cation "Ce^{4+}" is replaced by a trivalent one (Nd^{3+}). However, the subscript 2 has been maintained for the sake of simplicity.

2.2 Catalytic tests in a fix-bed reactor.

Catalytic tests were performed in a tubular quartz reactor coupled to specific NDIR-UV gas analyzers for CO, CO_2, NO, NO_2, SO_2 and O_2 monitoring (Fisher–Rosemount, models BINOS 100, 1001 and 1004). 20 mg of soot, 80 mg of catalyst, or 20 mg of soot + 80 mg of catalyst mixed in the so-called loose contact mode [18] were used in these experiments (and also an empty reactor). In all cases, the samples were diluted with 300 mg of SiC to avoid pressure drop and favor heat transfer. The model soot used in this study is a carbon black by Evonik-Degussa GmbH (Printex U).

Temperature programmed reactions were performed from room temperature until 700 ºC at 10 ºC/min with the gas mixtures $NOx/O_2/N_2$, $NOx/O_2/CO_2/N_2$, $NOx/O_2/H_2O/N_2$ and $NOx/O_2/SO_2/N_2$. Total flows of 500 ml/min were used (GHSV = 30000 h^{-1}), and the compositions of the different gases in these mixtures were 500 ppm NO (~ 0 ppm NO_2), 5 % O_2, 4 % CO_2, 2 % H_2O and 80 ppm SO_2 with N_2 balance.

Two additional soot combustion experiments were performed without any catalyst and with $Ce_{0.64}Zr_{0.27}Nd_{0.09}O_2$ under a $NOx/O_2/CO_2/H_2O/N_2$ gas flow. These experiments consisted of raising the temperature from room temperature until 530 ºC at 10 ºC/min, keeping the maximum temperature stable for 30 min.

137

138 *2.3 In situ DRIFTS* experiments.

139

140 A FTIR spectrometer (Jasco, model FT/IR-4100) was used for *in situ*
141 DRIFTS experiments, with a reaction cell that allows temperature and gas flow
142 composition control. The reactor is designated to allow the gas to flow through
143 the catalytic bed. The gas mixtures $NOx/O_2/N_2$, $NOx/O_2/CO_2/N_2$,
144 $NOx/O_2/H_2O/N_2$ and $NOx/O_2/SO_2/N_2$ were studied, with the same concentration
145 of the individual gases used in the previously described catalytic tests.

146 The experiments consisted of heating the catalysts (without soot) until
147 460 ºC under He flow, and a background spectrum was recorded in these
148 conditions for each catalyst. Then, the inert gas was replaced by the selected
149 reactive gas mixture and spectra were recorded after different times. The
150 background spectra have been subtracted in all spectra shown in this article,
151 and therefore, only bands attributed to adsorbed species are observed.

152

153 **3.- Results and discussion.**

154 *3.1. Catalytic tests in the fix-bed reactor.*

155 Figure 1 shows the soot conversion profiles obtained from CO + CO_2
156 evolved in combustion experiments performed with different gas mixtures,
157 where the effect of CO_2 (Figure 1b), H_2O (Figure 1c) and SO_2 (Figure 1d) in
158 soot oxidation under NOx and O_2 containing gas streams is analyzed.

159 As it was concluded in a previous study [17], both catalysts decrease the
160 soot combustion temperature with regard to the uncatalyzed reaction in the

161 $NOx/O_2/N_2$ gas mixture (Figure 1a), and $Ce_{0.64}Zr_{0.27}Nd_{0.09}O_2$ is more active than
162 $Ce_{0.73}Zr_{0.27}O_2$. The enhanced activity of the Ce-Zr mixed oxide upon Nd^{3+}
163 doping was attributed to the creation of oxygen vacancies, which improve the
164 redox properties of the mixed oxide

165 As a general trend, the presence of either CO_2 (Figure 1b), H_2O (Figure
166 1c) or SO_2 (Figure 1d), in addition to NOx and O_2, decrease the activity of both
167 catalysts with regard to the reaction under $NOx/O_2/N_2$ (Figure 1a), while
168 differences in the uncatalyzed reactions are not obvious for the different gas
169 mixtures tested. The strongest inhibitor effect on the catalyzed reactions is
170 attributed to SO_2, followed by H_2O and finally CO_2. On the other hand,
171 regardless the gas mixture used, the catalytic activity for soot combustion of
172 $Ce_{0.64}Zr_{0.27}Nd_{0.09}O_2$ is equal or higher to that of $Ce_{0.73}Zr_{0.27}O_2$.

173 In a previous study [17] performed with $Ce_{0.73}Zr_{0.27}O_2$ and
174 $Ce_{0.64}Zr_{0.27}Nd_{0.09}O_2$, and also in many others studies performed with different
175 soot combustion catalysts [6, 19, 20], the catalytic oxidation of NO to NO_2 was
176 identified as an important step in the catalyzed soot combustion mechanism,
177 since NO_2 is more oxidizing than NO and O_2. This is the so-called NO_2-assisted
178 soot combustion mechanism, where the catalyst accelerates the oxidation of
179 NO to NO_2, NO_2 ignites soot and O_2 is able to continue the combustion once
180 this has started. In order to explore the reasons of the inhibiting effects of CO_2,
181 H_2O and SO_2, the NO_2 profiles obtained in oxidation experiments performed
182 without (Figure 2) and with soot (Figure 3) have been analyzed.

183 All NO_2 profiles obtained in the absence of soot (Figure 2) are
184 qualitatively similar. In spite of thermodynamics predict that NO_2 should be the
185 main NOx component at low temperature, NO_2 concentration is null at the

186 beginning of the experiments. This is because the experimental set-up used in
187 this study has been designed to minimize the gas phase oxidation of NO to NO_2
188 before the reactor, in order to mimic real diesel exhausts.

189 Both catalysts accelerate the oxidation of NO to NO_2 in all the gas
190 mixtures until the thermodynamic equilibrium is achieved at a certain
191 temperature, which has been defined as $T_{max}NO_2$, and above this temperature
192 NO_2 decreases following the thermodynamic equilibrium. Both the catalyst
193 nature and the gas mixture affect the onset NO oxidation temperature (which is
194 not shown in all curves of Figure 3 for clarity), the $T_{max}NO_2$ and the maximum
195 NO_2 level achieved.

196 In accordance with the soot combustion experiments (Figure 1a),
197 $Ce_{0.64}Zr_{0.27}Nd_{0.09}O_2$ accelerates NO_2 production more efficiently than
198 $Ce_{0.73}Zr_{0.27}O_2$ in the $NOx/O_2/N_2$ gas mixture (Figure 2a). On the contrary,
199 $Ce_{0.73}Zr_{0.27}O_2$ is more active than $Ce_{0.64}Zr_{0.27}Nd_{0.09}O_2$ under $NOx/O_2/CO_2/N_2$
200 (Figure 2b) and $NOx/O_2/SO_2/N_2$ (Figure 2d), and both catalysts behave equal
201 under $NO/O_2/H_2O/N_2$ (Figure 2c). This means that there is not a direct
202 relationship between NO_2 production and soot combustion in this case, as it will
203 be discussed in detail afterwards, in spite of the catalytic oxidation of NO to NO_2
204 is one of the reactions involved in the soot combustion mechanism. This is
205 confirmed by the shape of the NO_2 profiles obtained in the presence of soot
206 (Figure 3), which is different to that obtained in the absence of soot because
207 part of the NO_2 produced by catalytic oxidation of NO is consumed by the NO_2-
208 soot reaction. The main nitrogen product of the NO_2-carbon reaction is NO, and
209 therefore net NOx (= NO + NO_2) removal is quite low. NOx removal curves are

included in Figure 1SM of the supplementary material, where it is shown that NOx removal level is always lower than 10%.

As a summary, the catalytic oxidation of NO to NO_2 is one of the reactions involved in the soot combustion mechanism in all the gas mixtures tested, and the inhibiting effect of the gases tested on both NO_2 production and soot combustion follows the trend: $SO_2 > H_2O > CO_2$. However, if the behavior of both catalysts towards NO_2 production and soot combustion is compared, it is concluded that soot combustion not only depends on NO_2 production. In order to analyze this in more detail, the relationship between soot combustion (represented by the T50% (ºC) temperatures determined from Figure 1) and NO_2 production (represented by the Tmax NO_2 (ºC) determined from Figure 2) is plotted on Figure 4. Quite linear relationships are obtained for both catalysts, but data obtained with $Ce_{0.73}Zr_{0.27}O_2$ are always above those obtained with $Ce_{0.64}Zr_{0.27}Nd_{0.09}O_2$. This confirms that NO_2 production is actually a key step in the catalytic combustion of soot. However, for similar NO_2 production, $Ce_{0.64}Zr_{0.27}Nd_{0.09}O_2$ is more effective for soot combustion than $Ce_{0.73}Zr_{0.27}O_2$, and this suggests the additional participation of the “active oxygen” mechanism in the soot combustion reactions. It is known that ceria-catalysts are able to exchange oxygen with gas phase O_2 molecules [21-23], and deliver highly reaction active oxygen species to soot, and also to NO to be oxidized to NO_2. This additional mechanism would explain the differences between $Ce_{0.64}Zr_{0.27}Nd_{0.09}O_2$ and $Ce_{0.73}Zr_{0.27}O_2$, since the introduction of Nd^{3+} on the Ce-Zr mixed oxide improves the oxide reducibility and favors vacant sites formation, [17] and these improvements promote active oxygen production. Therefore, Nd^{3+} doping is expected to promote the participation of the active

oxygen mechanism besides the NO_2-assisted mechanism in the catalytic combustion of soot.

It is worthy paying attention to the lower NO_2 levels detected during the $Ce_{0.64}Zr_{0.27}Nd_{0.09}O_2$-catalysed soot combustion experiments in all the gas mixtures tested (see Figures 3a, 3b and 3c), except in $NOx/O_2/SO_2/N_2$. These NO_2 levels are lower than those obtained with $Ce_{0.73}Zr_{0.27}O_2$, regardless the NO_2 production capacity measured in the absence of soot (Figure 2). This means that NO_2 is used more efficiently during the $Ce_{0.64}Zr_{0.27}Nd_{0.09}O_2$-catalysed soot combustion than when $Ce_{0.73}Zr_{0.27}O_2$ catalyzes the reaction, which is also related to the important role of the “active oxygen” mechanism. Once the active oxygen of $Ce_{0.64}Zr_{0.27}Nd_{0.09}O_2$ reacts with soot, the remaining oxidizing gases in the mixture, mainly NO_2 and O_2, react more easily, and this produces a synergetic effect between the high oxidation capacities of NO_2 and active oxygen. This would explain why NO_2 is used more efficiently by $Ce_{0.64}Zr_{0.27}Nd_{0.09}O_2$.

Finally, soot combustion experiments where performed in a gas mixture that simulates a real diesel engine exhaust, including NOx, O_2, H_2O, CO_2 and N_2 (Figure 5 and Table 1). SO_2 has not been included in this gas mixture because the poisoning effect of this gas inhibits almost completely the activity of the catalysts studied (see Figure 1d), and therefore, it is assumed that the ceria-based catalysts can be only used for catalytic combustion of soot on engines running with sulfur-free diesel fuel. These additional soot combustion experiments have been performed with $Ce_{0.64}Zr_{0.27}Nd_{0.09}O_2$, which is the most active ceria catalyst tested in this study, and without catalyst. The maximum temperature achieved is 530 ºC, which is about the maximum temperature that

can be reached in a real diesel exhaust using high engine loading and fitting the soot filter just at the exit of the engine [24]. As it was previously mentioned, higher temperatures can be reached in hot spots inside the filters during regeneration, but simulating these transient conditions is out the scope of this study. The only precaution taken in the current study was to calcine catalysts at 800 ºC in order to provide thermal stability and practical interest to the oxides used.

Both the uncatalyzed and catalyzed reactions started at 450 ºC in this complex gas stream. However, the uncatalyzed reaction stopped after 23 % soot combustion, while not the catalyzed combustion. This can be explained by the fact that the structure of the model soot used (and also of typical real soots) consists of a turbulent core surrounded by spherical graphitic carbon layers forming an onion-like structure [25-30]. The surface of the soot particles is more reactive than the more internal well-ordered graphitic layers due to the presence of adsorbed hydrocarbons (the volatile matter of the model soot used in this study amounts to 8%). The O_2 molecule, which is the main responsible of the uncatalyzed combustion, is only able to oxidize part of the soot sample and the reaction stops once the most reactive part of the soot particles is consumed. On the contrary, both NO_2 and catalyst active oxygen assist O_2 during the $Ce_{0.64}Zr_{0.27}Nd_{0.09}O_2$-catalysed soot combustion, and the higher reactivity of these species allows further soot combustion. Also, the maximum soot combustion rate achieved during the catalyzed reaction is about three times higher than that of the uncatalyzed combustion, and $Ce_{0.64}Zr_{0.27}Nd_{0.09}O_2$ also improves the CO_2 selectivity (see data on Table 1). The improved CO_2

selectivity can be attributed either to the selective formation of this gas as primary gas product or to the catalytic oxidation of the CO first evolved.

3.2. In situ DRIFTS experiments.

In order to analyze the reasons of the partial or total inhibiting effect of H_2O, CO_2 and SO_2, *in situ* DRIFTS experiments have been performed at 460 ºC. The nature of the species adsorbed on the catalysts' surface has been analyzed, and due to this reason, these experiments have been carried out without soot (only with the catalysts). Representative spectra obtained with both catalysts under the different gas mixtures evaluated are included in the Figure 2SP (supplementary material), covering the entire range of wavenumbers measured (4000-500 cm^{-1}). Most relevant bands for the purpose of this study appear in the 1800-1000 cm^{-1} range, and the further analysis and discussion of the spectra is focused on this range of wavenumbers.

Figure 6 shows the spectra obtained under the $NOx/O_2/N_2$ atmosphere with $Ce_{0.73}Zr_{0.27}O_2$ (Figure 6a) and $Ce_{0.64}Zr_{0.27}Nd_{0.09}O_2$ (Figure 6b) in the 1800-1000 cm^{-1} range, where bands of nitrogen-containing surface groups appear. These spectra (and some others) were included and discussed in detail in a previous study, and a complete interpretation was there reported [17]. However, it seems convenient to include also a brief discussion of the behavior of these catalysts in the $NOx/O_2/N_2$ atmosphere in this article for further comparison with more complex gas mixtures. Two intense adsorption bands that grow with time are observed on $Ce_{0.73}Zr_{0.27}O_2$ (Figure 6a) and $Ce_{0.64}Zr_{0.27}Nd_{0.09}O_2$ (Figure 6b)

spectra. These bands are located in the 1650-1450 cm^{-1} and 1350-1150 cm^{-1} ranges, and are consistent with the presence of nitrates and nitrites + nitrates, respectively [31]. Several well-defined peaks appear at particular wavenumbers within the two main bands of the $Ce_{0.73}Zr_{0.27}O_2$ and $Ce_{0.64}Zr_{0.27}Nd_{0.09}O_2$ spectra, and this is attributed to the presence of nitrites and/or nitrates with different configuration (monodentate, bidentate and/or bridged) adsorbed on different surface sites of the heterogeneous surface of these catalysts. In both figures (Figures 6a and 6b), the band which is unambiguously assigned to nitrate species (1650-1450 cm^{-1} range) is the most intense, and the relative intensity of the band at 1350-1150 cm^{-1} with regard to that at 1650-1450 cm^{-1} can be related with the presence of nitrites. The relative intensity of the band at 1350-1150 cm^{-1} is higher for the $Ce_{0.64}Zr_{0.27}Nd_{0.09}O_2$ catalyst (Figure 6b) than for $Ce_{0.73}Zr_{0.27}O_2$ (Figure 6a), suggesting that Nd^{3+} doping favors the formation of nitrites. Nitrites are less oxidized species than nitrates, and its formation on the Nd^{3+}-containing oxide is consistent with the creation of oxygen vacancies due to the substitution of tetravalent Ce^{4+} cations by trivalent Nd^{3+} cations. Also, nitrites have inferior thermostability than nitrates and decompose more easily [32], and this would explain why Nd^{3+} doping slightly improves the NO_2 production capacity of the Ce-Zr mixed oxide in the $NOx/O_2/N_2$ atmosphere (see Figure 2a). Nd^{3+} promotes the formation of less stable surface nitrogen species and provides and alternative and faster NO_2 production pathway.

3.2.1. CO_2 effect.

The bands attributed to nitrates (1650-1450 cm^{-1}) and nitrites + nitrates (1350-1150 cm^{-1}) [31] are also observed in the spectra obtained with the gas mixture $NOx/O_2/CO_2/N_2$, both for $Ce_{0.73}Zr_{0.27}O_2$ (Figure 7a) and $Ce_{0.64}Zr_{0.27}Nd_{0.09}O_2$ (Figure 7b). However, an additional signal appears around 1400 cm^{-1}, between both bands assigned to nitrogen compounds.

Various carbonate-type species have been reported to present adsorption modes in the range 1200-1600 cm^{-1}. A band at ca. 1478 cm^{-1} has been proposed to correspond to the antisymmetric stretching of the terminal C-O bonds in poly or monodentate carbonates, and the corresponding symmetric mode would appear at ca. 1350 cm^{-1} [33, 34]. Bands of hydrogen carbonate (at 1214, 1399–1410 and ca. 1600 cm^{-1}) and bidentate carbonate (bands at ca. 1583 and 1297 cm^{-1}) would appear in this range of wavenumbers as well [33-35].

The spectra obtained including CO_2 in the gas mixture (Figure 7) evidence the formation of carbonate species on both catalysts, but a detailed identification of the type of carbonate specie formed is not possible because some of the bands overlap with those of the nitrogen surface groups. However, it seems reasonable to rule out the formation of hydrogen carbonates, because this would require the participation of hydroxyl groups (or water). Hydroxyl groups may be detected by DRIFTS bands in the 4000-3000 cm^{-1} range, and their potential consumption upon CO_2 chemisorption and hydrogen carbonates formation may be evidenced by negative bands in this range of wavenumbers. These evidences have not been observed in our spectra (see Figure 2SM of the supplementary material). The absence of hydroxyl groups on the catalysts studied must be attributed to the high calcination temperature used (800 ºC). It

357 is therefore presumed the formation of carbonate species on both catalysts
358 during the *in situ* DRIFTS experiments performed under $NOx/O_2/CO_2/N_2$.

359 The chemisorption of CO_2 on the catalysts modifies the nature of the
360 nitrogen surface species, mainly affecting the formation of nitrites on
361 $Ce_{0.64}Zr_{0.27}Nd_{0.09}O_2$ (Figure 7b). For this catalyst, the ratio between the DRIFT
362 signal at 1547 cm^{-1}, which is attributed to nitrates, and that at 1242 cm^{-1}, which
363 is assigned to nitrites + nitrates, after 60' on the gas streams increases from 2.0
364 for $NOx/O_2/N_2$ to 2.5 for $NOx/O_2/CO_2/N_2$. This indicates that CO_2 chemisorption
365 hinders the formation of nitrites on $Ce_{0.64}Zr_{0.27}Nd_{0.09}O_2$, and nitrites were
366 proposed to be reaction intermediates of the fast catalytic oxidation of NO to
367 NO_2 on $Ce_{0.64}Zr_{0.27}Nd_{0.09}O_2$. This would explain the important decrease of the
368 NO_2 formation under $NOx/O_2/CO_2/N_2$ with regard to $NOx/O_2/N_2$ for experiments
369 performed with $Ce_{0.64}Zr_{0.27}Nd_{0.09}O_2$ (compare Figures 2a and 2b). However, the
370 effect of CO_2 on the nature of the nitrogen surface species is not so relevant for
371 the $Ce_{0.73}Zr_{0.27}O_2$ catalyst (compare Figures 6a and 7a), and neither is on the
372 $Ce_{0.73}Zr_{0.27}O_2$-catalysed oxidation of NO to NO_2 (compare Figures 2a and 2b).

373 In conclusion, CO_2 and NOx compete for the adsorption sites on the
374 catalysts' surface, and mainly for the Nd^{3+}-containing catalyst, this affects the
375 catalytic oxidation of NO to NO_2. However, the soot combustion experiments
376 (Figure 1b) evidence that, although the $Ce_{0.64}Zr_{0.27}Nd_{0.09}O_2$-catalysed NO
377 oxidation is impeded, the catalytic combustion of soot remains faster than with
378 $Ce_{0.73}Zr_{0.27}O_2$. This supports the hypothesis of the important contribution of the
379 active oxygen mechanism during the $Ce_{0.64}Zr_{0.27}Nd_{0.09}O_2$-catalysed soot
380 combustion, which seems to remain relevant even after the partial inhibition of
381 the NO_2-assisted soot combustion mechanism by CO_2 chemisorption.

382

383 *3.2.2. H_2O effect.*

384

385 The DRIFT spectra obtained under the $NOx/O_2/H_2O/N_2$ gas stream with
386 the $Ce_{0.73}Zr_{0.27}O_2$ and $Ce_{0.64}Zr_{0.27}Nd_{0.09}O_2$ catalysts are compiled in Figures 8a
387 and 8b, respectively. The bands attributed to nitrates (1650-1450 cm^{-1}) and
388 nitrites + nitrates (1350-1150 cm^{-1}) [31] are also observed in the spectra
389 obtained with this gas mixture. The presence of water in the gas mixture delays
390 the formation of the nitrogen surface groups (compare Figures 6 ($NOx/O_2/N_2$)
391 and 8 ($NOx/O_2/H_2O/N_2$)), and this delay affects both catalysts. For instance,
392 bands of significant intensity appear after 1 minute under reaction conditions in
393 the absence of H_2O (Figure 6), while not in the presence of H_2O (Figure 8). The
394 reason of this delay is expected to be the competition between H_2O and NOx
395 for the adsorption sites on the catalysts' surface. H_2O chemisorption should
396 form hydroxyl groups, but evidences of this type of groups are not observed in
397 the 4000-3000 cm^{-1} region (see Figure 2SM in supplementary material). This is
398 because hydroxyl groups are suitable sites for NOx chemisorption, as
399 previously observed [32], and it seems they are depleted by NOx chemisorption
400 as soon as they are formed. According to this interpretation H_2O would force the
401 catalytic oxidation of NO to NO_2 to progress through a different and slower
402 reaction pathway than that occurring in the absence of H_2O. This would explain
403 why the presence of H_2O in the gas mixture diminishes the catalytic oxidation of
404 NO to NO_2 (compare Figures 2a ($NOx/O_2/N_2$) and 2c ($NOx/O_2/H_2O/N_2$)) and the
405 catalytic combustion of soot (compare Figures 1a ($NOx/O_2/N_2$) and 1c
406 ($NOx/O_2/H_2O/N_2$)), but not inhibits completely the reactions as SO_2 almost does.

An additional argument to support this interpretation is obtained by the detailed analysis of the spectra in the 1650-1450 cm^{-1} range (Figure 8), which is attributed to nitrates. Nitrates can be adsorbed on a solid surface in different configurations of different stability, and the actual position of the adsorption bands of each type of nitrate is different. These configurations are, in increasing order of stability: monodentate nitrates, bidentate nitrates and bridging nitrates, and it has been reported they present adsorption bands in the 1530–1480 cm^{-1}, 1565–1500 cm^{-1} and 1650–1600 cm^{-1} ranges, respectively [31]. As deduced from this assignation, the higher the stability of a surface nitrate specie, the higher the absorption band wavenumber in this interval.

Different contributions to the bands in the 1650-1450 cm^{-1} range are observed on Figures 6 ($NOx/O_2/N_2$) and 8 ($NOx/O_2/H_2O/N_2$) due to the presence of different surface nitrate species. For instance, the main band in this region obtained with the $Ce_{0.73}Zr_{0.27}O_2$ catalyst under $NOx/O_2/N_2$ appears at 1527 cm^{-1} (see Figure 6a), and therefore, it can be attributed to monodentate or bidentate nitrates. In addition, some other contributions appear with lower intensity at higher wavenumbers (1547 and 1559 cm^{-1}), which can be assigned to bidentate and/or bridging nitrates. Bands at quite similar wavenumbers are also observed in the presence or H_2O with the $Ce_{0.73}Zr_{0.27}O_2$ catalyst (Figure 8a; $NOx/O_2/H_2O/N_2$), but the relative intensity of the most stable species (bidentate and bridging nitrates) is higher, and a new contribution assigned to bridging nitrates appears at 1594 cm^{-1}. This supports that the presence of H_2O favors the formation of more stable nitrate species with regard to those formed in its absence, and this applies to the two catalysts studied.

In conclusion, the presence of water in the gas mixture hinders the catalytic oxidation of NO to NO_2, and therefore the catalytic combustion of soot, because it delays the formation of reaction intermediates on the catalyst surface and favors the formation of more stable nitrogen surface groups than in a H_2O-free gas stream.

3.2.3. SO_2 effect.

Finally, the effect of SO_2 has also been studied by DRIFTS, and the spectra are included on Figure 9 for $Ce_{0.73}Zr_{0.27}O_2$ (Figure 9a) and $Ce_{0.64}Zr_{0.27}Nd_{0.09}O_2$ (Figure 9b).

Important differences have been noticed in these experiments performed under $NOx/O_2/SO_2/N_2$ with regard to the previously studied gas mixtures. In the presence of SO_2, the nitrates bands at 1650-1450 cm^{-1} grow once the gas mixture is put in contact with the catalysts, but they decrease afterwards. Also the nitrites + nitrates band (1350-1150 cm^{-1}) of the $Ce_{0.73}Zr_{0.27}O_2$ catalyst (Figure 9a) grows with time, but much more slowly than in the absence of SO_2 (compare with Figure 6a). In addition to these changes in the behavior of the nitrogen surface groups, a prominent band grows at 1348 cm^{-1} on the $Ce_{0.73}Zr_{0.27}O_2$ catalyst (Figure 9a), which is progressively shifted to 1376 cm^{-1}. This band appears at 1345 cm^{-1} on the $Ce_{0.64}Zr_{0.27}Nd_{0.09}O_2$ catalyst (Figure 9b), but with much lower intensity. This band has been assigned to a S=O vibration mode of surface sulfates or adsorbed SO_3 [36-38]. A new band at 1293 cm^{-1} grows on the $Ce_{0.73}Zr_{0.27}O_2$ catalyst (Figure 9a) as well, which has been also assigned to sulfate species [36].

These experiments evidence that SO_2 and NOx compete by the surface adsorption sites, and sulfates formation significantly inhibits the catalytic oxidation of NO to NO_2 (compare Figures 2a ($NOx/O_2/N_2$) and 2d ($NOx/O_2/SO_2/N_2$)), and at the end, the catalytic combustion of soot (compare Figures 1a ($NOx/O_2/N_2$) and 1d ($NOx/O_2/SO_2/N_2$)).

According to the important differences observed in the DRIFT spectra obtained in the presence of SO_2 for both catalysts (see Figure 9), sulfate formation seems to affect much more to $Ce_{0.73}Zr_{0.27}O_2$ than to $Ce_{0.64}Zr_{0.27}Nd_{0.09}O_2$, but the effect on the catalytic oxidation of NO to NO_2 is stronger for $Ce_{0.64}Zr_{0.27}Nd_{0.09}O_2$ (see Figure 2d). This suggest that the catalytic oxidation of NO to NO_2 is not only related with the nitrogen surface groups observed by DRIFTS but active oxygen, which cannot be observed so far, seems to be also involved in the catalytic oxidation of NO and seems to be also affected by SO_2 chemisorption. This would explain why the $Ce_{0.64}Zr_{0.27}Nd_{0.09}O_2$ catalyst, whose catalytic activity not only depends on NO_2 formation but also on active oxygen production (see Figure 4 and the discussion on the text), suffer the same SO_2 inhibiting effect than $Ce_{0.73}Zr_{0.27}O_2$ in spite of the important differences on the nitrogen surface groups behavior observed by DRIFTS (see Figure 9).

4.- Conclusions.

The effect of CO_2, H_2O and SO_2 in the $Ce_{0.73}Zr_{0.27}O_2$ and $Ce_{0.64}Zr_{0.27}Nd_{0.09}O_2$-catalyzed combustion of soot in the presence of NOx and O_2 has been studied, and the main conclusions achieved can be summarized as follows:

- The presence of CO_2, H_2O or SO_2, in addition to NOx and O_2, in the gas mixture decreases the activity for soot combustion of both catalysts with regard to the combustion in a $NOx/O_2/N_2$ mixture. The inhibiting effect follows the trend $SO_2 > H_2O > CO_2$.

- CO_2 partially inhibits the catalytic activity because competes with NOx for the adsorption sites on the catalysts' surface, and mainly for the Nd^{3+}-containing catalyst, this affects the catalytic oxidation of NO to NO_2. However, the $Ce_{0.64}Zr_{0.27}Nd_{0.09}O_2$-catalysed combustion of soot remains faster, and this is attributed to the contribution of the active oxygen mechanism.

- The presence of H_2O in the gas mixture hinders the catalytic oxidation of NO to NO_2 on both catalysts, and therefore the catalytic combustion of soot, because it delays the formation of reaction intermediates on the catalyst surface and favors the formation of more stable nitrogen surface groups than in a H_2O -free gas stream.

- SO_2 and NOx also compete by the surface adsorption sites on the catalysts, and sulfates formation significantly inhibits the catalytic oxidation of NO to NO_2, and at the end, the catalytic combustion of soot. The high stability of sulfates explains the strongest inhibiting effect of SO_2.

- Regardless the gas mixture used the catalytic activity for soot combustion of $Ce_{0.64}Zr_{0.27}Nd_{0.09}O_2$ is equal or higher to that of $Ce_{0.73}Zr_{0.27}O_2$, and it is proposed that this is because Nd^{3+} doping promotes the participation of the active oxygen mechanism together with the NO_2-assisted mechanism in the catalytic combustion of soot.

- The maximum soot combustion rate achieved during a $Ce_{0.64}Zr_{0.27}Nd_{0.09}O_2$-catalyzed reaction in $NOx/O_2/CO_2/H_2O/N_2$ is about three times higher than that of the uncatalyzed combustion, and this catalyst also improves the CO_2 selectivity.

Acknowledgments

The authors thank the financial support of Generalitat Valenciana (Project Prometeo 2009/047), the Spanish Ministry of Economy and Competitiveness (Project CTQ2012-30703), and the UE (FEDER funding).

References

[1] S. Liu, X. Wu, D. Weng, M. Li, J. Fan, Appl. Catal. B 138-139 (2013) 199–211.

[2] Y. Wei, J. Liu, Z. Zhao, A. Duan, G. Jiang, J. Catal. 287 (2012) 13–29.

[3] M. V. Twigg. Appl. Catal. B 70 (2007) 2–15.

[4] E. Aneggi, C. de Leitenburg, G. Dolcetti, A. Trovarelli, Catal. Today 114 (2006) 40–47.

[5] A. M. Hernández-Giménez, D. Lozano Castelló, A. Bueno-López, Chem. papers (2013). DOI 10.2478/s11696-013-0469-7

[6] J. Oi Uchisawa, A. Obuchi, Z. Zhao, S. Kushiyama, Appl. Catal. B 18 (1998) L183-L187.

[7] J. Oi-Uchisawa, A. Obuchi, R. Enomoto, S. Liu, T. Nanba, S. Kushiyama, Appl. Catal. B 26 (2000) 17–24.

[8] J. Oi-Uchisawa, S. Wang, T. Nanba, A. Ohi, A. Obuchi, Appl. Catal. B 44 (2003) 207–215.

[9] A. Bueno-López, Appl. Catal. B 146 (2014) 1– 11

[10] M. Dhakad, T. Mitshuhashi, S. Rayalu, Pradip Doggali, S. Bakardjiva, J. Subrt, D. Fino, H. Haneda, N. Labhsetwar, Catal. Today 132 (2008) 188–193.

[11] M. Machida, Y. Murata, K. Kishikawa, D. Zhang, K. Ikeue, Chem. Mater. 20 (2008) 4489–4494.

[12] R. Flouty, E. Abi-Aad, S. Siffert, A. Aboukaıs, Appl. Catal. B 46 (2003) 145–153.

[13] D. Weng, J. Li, X. Wu, F. Lin, Catal. Commun. 9 (2008) 1898–1901.

[14] M.A. Peralta, V.G. Milt, L.M. Cornaglia, C.A. Querini, J. Catal. 242 (2006) 118–130.

[15] K. Tikhomirov, O. Krocher, M. Elsener, A. Wokaun, Appl. Catal. B 64 (2006) 72–78.

[16] I. Atribak, A. Bueno-López, A. García-García, J. Catal. 259 (2008) 123–132.

[17] A. M. Hernández-Giménez, L. P. dos Santos Xavier, A. Bueno-López, Appl. Catal. A 462–463 (2013) 100–106.

[18] B.A.A.L. van Setten, J.M. Schouten, M. Makkee, J.A. Moulijn, Appl. Catal. B 28 (2000) 253–257.

[19] A. Setiabudi, B.A.A.L. van Setten, M. Makkee, J. A. Moulijn, Appl. Catal. B 35 (2002) 159–166.

[20] A. Setiabudi, M. Makkee, Jacob A. Moulijn, Appl. Catal. B 50 (2004) 185–194

[21] A. Bueno-López, K. Krishna, M. Makkee, J.A. Moulijn, J. Catal. 230 (2005) 237–248.

[22] A. Bueno-López, K. Krishna, B. van der Linden, G. Mul, J.A. Moulijn, M. Makkee, Catal. Today 121 (2007) 237–245.

[23] N. Guillén-Hurtado, A. García-García, A. Bueno-López, J. Catal. 299 (2013) 181–187.

[24] M. Valencia, E. López, S. Andrade, Iris M.L., N. Guillén Hurtado, V. Rico Pérez, A. García García, C. Salinas Martínez de Lecea, A. Bueno López, Top. Catal. (2013) 56:452–456.

[25] J.P.A. Neeft, M. Makkee, J.A. Moulijn, Fuel Proc. Technol. 47 (1996) 1.

[26] B.A.A.L. van Setten, M. Makkee, J.A. Moulijn, Catal. Rev. Sci. Eng. 43 (2001) 489.

[27] B.R. Stanmore, J.F. Brilhac, P. Gilot, Carbon 39 (2001) 2247–2268.

[28] M.M. Maricq, Aerosol Sci. 38 (2007) 1079.

[29] I. Atribak, A. Bueno-López, A. García-García, Comb. Flame 157 (2010) 2086–2094.

[30] F. E. López Suárez, A. Bueno-López, M. J. Illán-Gómez, B. Ura, J. Trawczynski, Catal. Today 176 (2011) 182–186.

[31] K. I. Hadjiivanov, Catal. Rev. Sci. Eng., 42 (2000) 71-144.

[32] I. Atribak, B. Azambre, A. Bueno López, A. García-García, Appl. Catal. B 92 (2009) 126-137.

[33] D. Gamarra, A. Martínez-Arias, J. Catal. 263 (2009) 189–195.

[34] C. Binet, M. Daturi, J.-C. Lavalley, Catal. Today 50 (1999) 207.

[35] O. Pozdnyakova, D. Teschner, A. Wootsch, J. Kröhnert, B. Steinhauer, H. Sauer, L. Toth, F.C. Jentoft, A. Knop-Gericke, Z. Paál, R. Schlögl, J. Catal. 237 (2006) 1.

[36] F. Babou, G. Coudurier, J. C. Vedrine, J. Catal. 152 (1995) 341-349.

[37] B. Azambre, L. Zenboury, J.V. Weber, P. Burg, Appl. Surf. Sci. 256 (2010) 4570–4581.

[38] B. Azambre, L. Zenboury, P. Da Costa, S. Capela, S. Carpentier, A. Westermann, Catal. Today 176 (2011) 242– 249.

Table 1. Results of the soot combustion experiments in a $NOx/O_2/H_2O/CO_2/N_2$ atmosphere (curves on Figure 5).

Catalyst	**Burn off (%)**	**CO (%) = 100·CO/COx**	**Maximum rate (µgC/s)**
None	23	60	4
$Ce_{0.64}Zr_{0.27}Nd_{0.09}O_2$	73	19	10.5

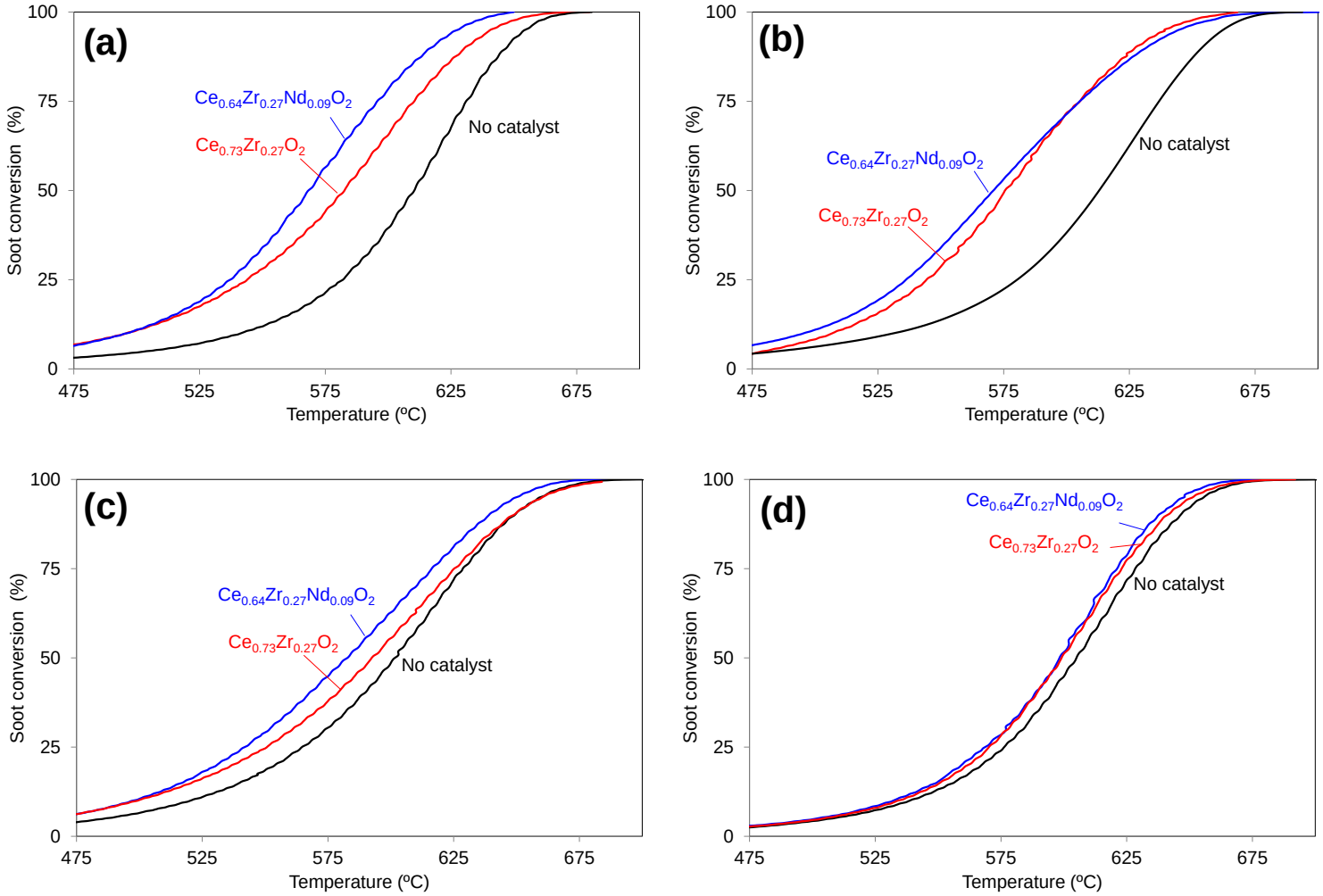

Figure 1. Soot combustion experiments performed under different gas mixtures: (a) $NOx/O_2/N_2$, (b) $NOx/O_2/CO_2/N_2$, (c) $NOx/O_2/H_2O/N_2$, (d) $NOx/O_2/SO_2/N_2$.

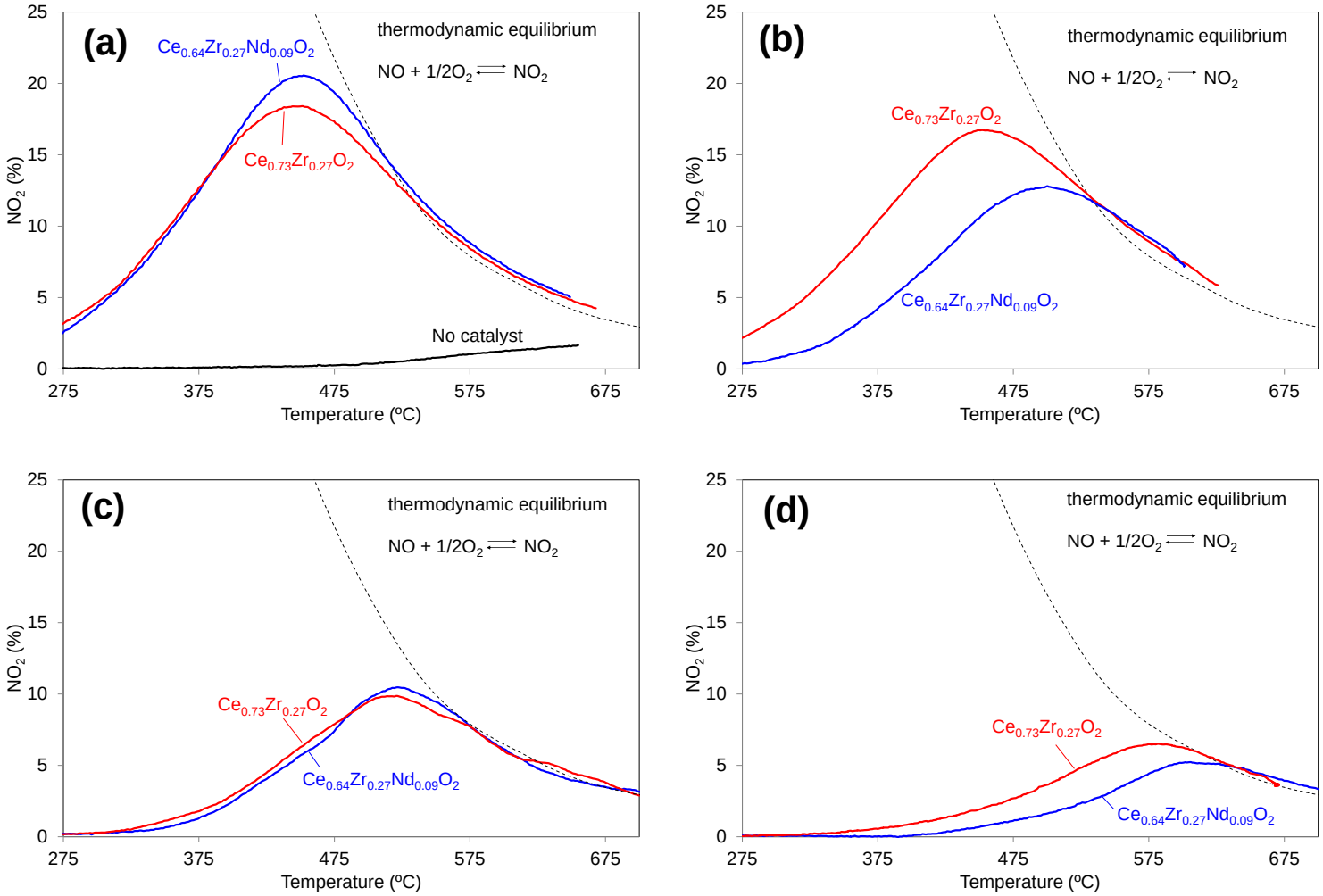

Figure 2. NO_2 formation in oxidation experiments performed without soot under different gas mixtures: (a) $NOx/O_2/N_2$, (b) $NOx/O_2/CO_2/N_2$, (c) $NOx/O_2/H_2O/N_2$, (d) $NOx/O_2/SO_2/N_2$.

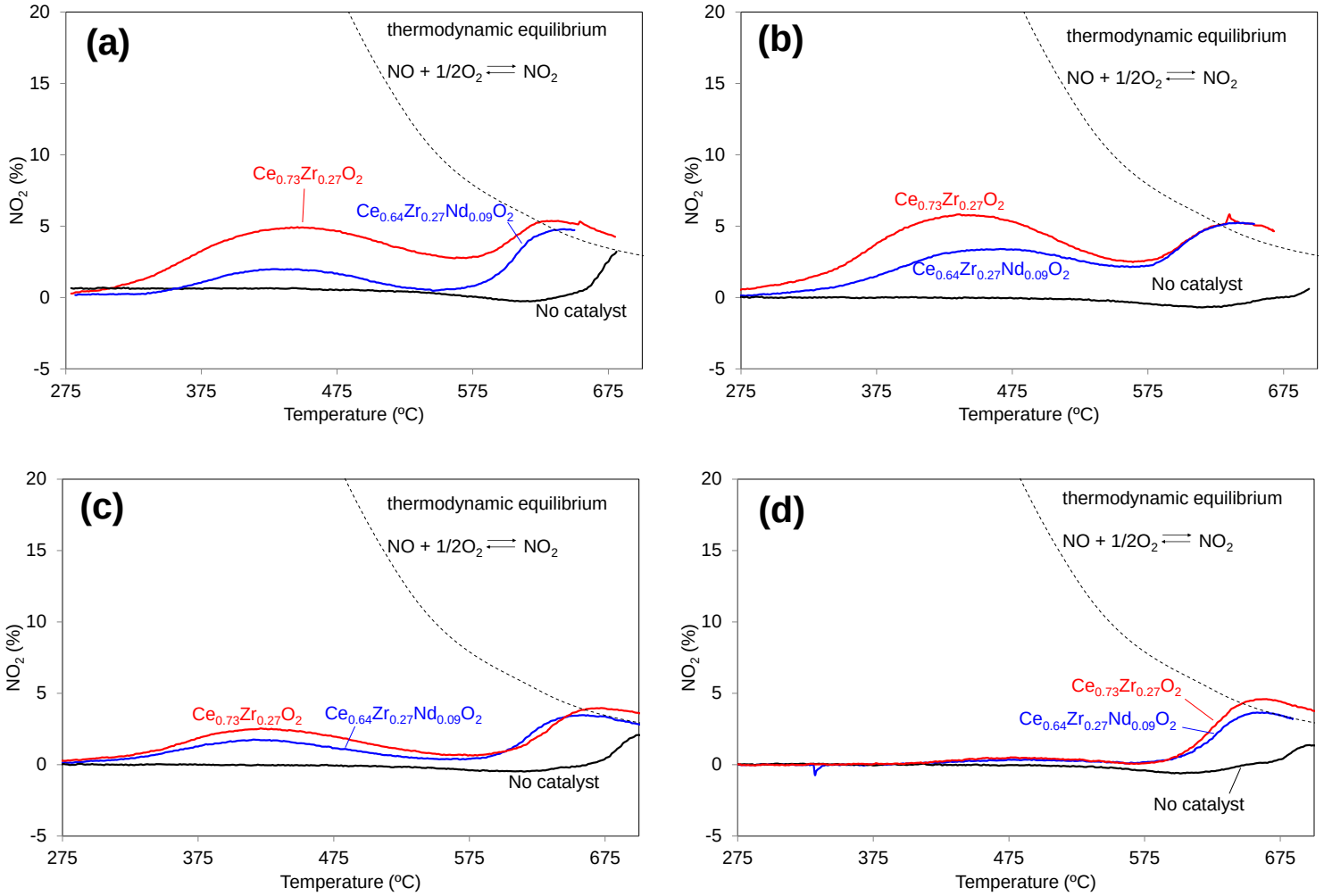

Figure 3. NO_2 formation in oxidation experiments performed with soot under different gas mixtures: (a) $NOx/O_2/N_2$, (b) $NOx/O_2/CO_2/N_2$, (c) $NOx/O_2/H_2O/N_2$, (d) $NOx/O_2/SO_2/N_2$. (These curves were obtained in the same experiments than soot conversion curves on Figure 1)

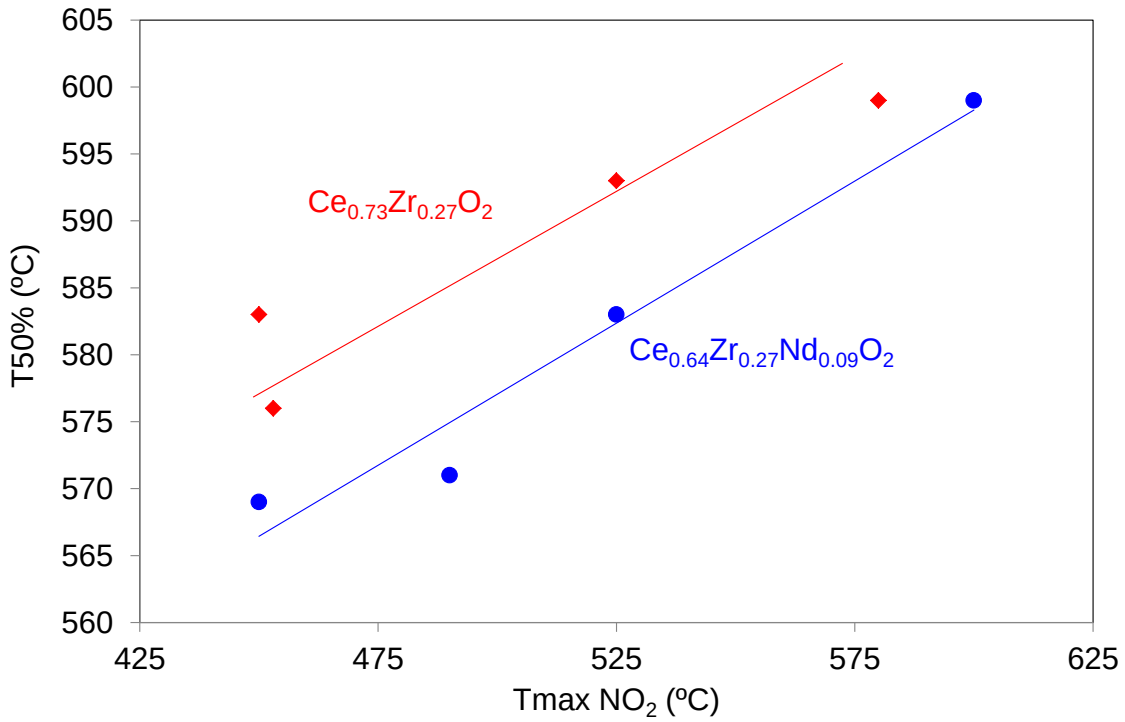

Figure 4. Relationship between soot combustion and NO_2 production. T50% (ºC): Temperature for 50% soot combustion; Tmax NO_2 (ºC): Temperature of maximum NO_2 production in blank experiments.

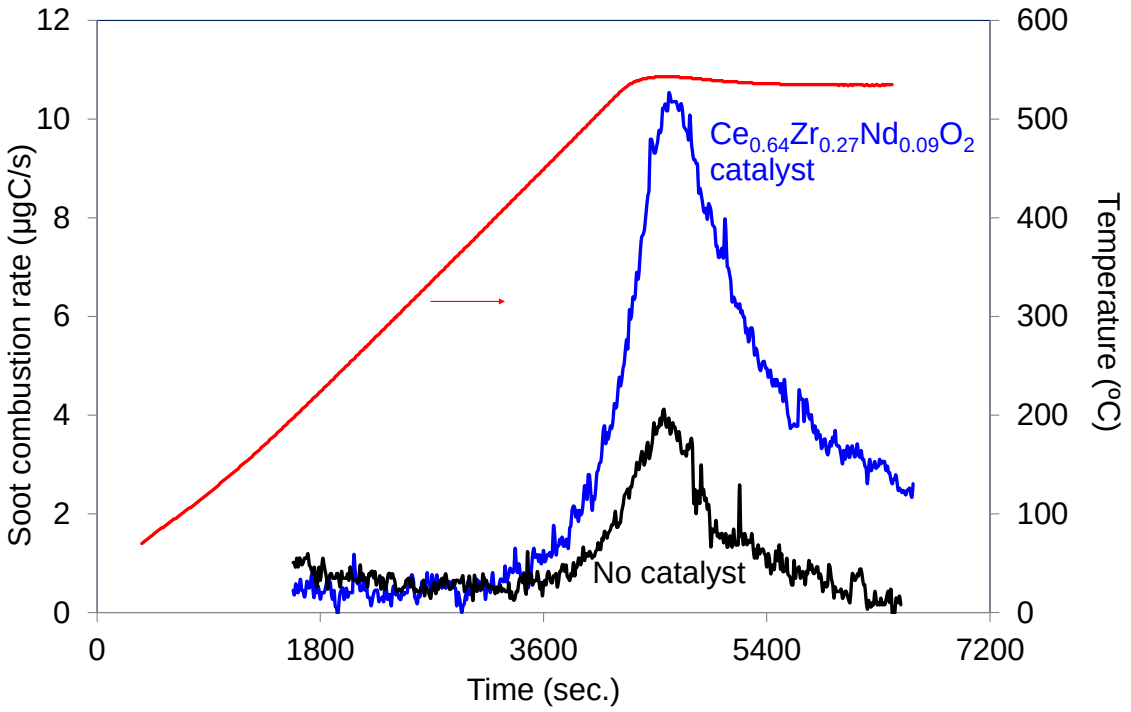

Figure 5. Soot combustion experiments in $NOx/O_2/H_2O/CO_2/N_2$.

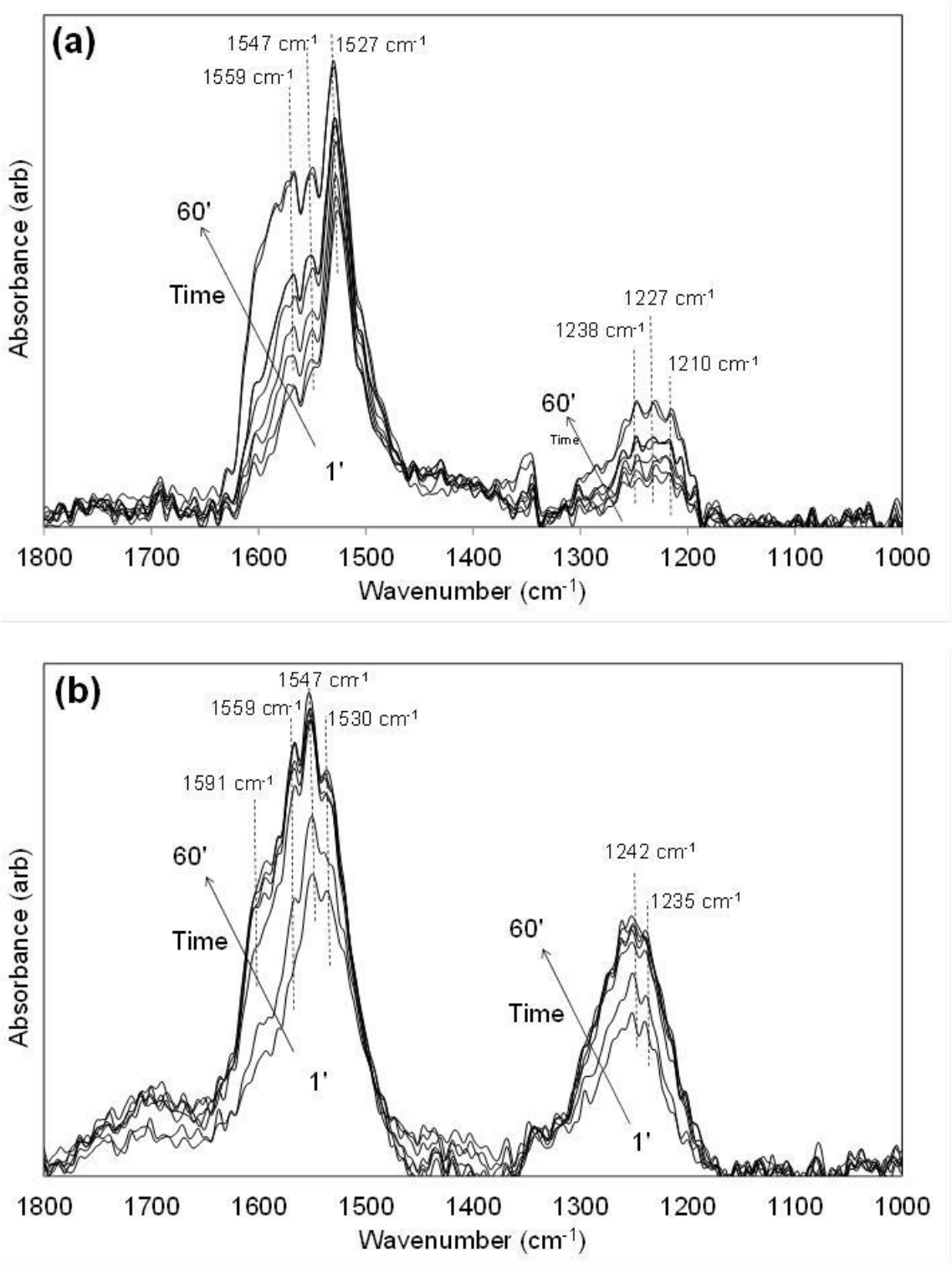

Figure 6. DRIFT spectra obtained in a $NOx/O_2/N_2$ atmosphere with (a) $Ce_{0.73}Zr_{0.27}O_2$ and (b) $Ce_{0.64}Zr_{0.27}Nd_{0.09}O_2$. (These Figures have been reprinted from [17] for the sake of clarity).

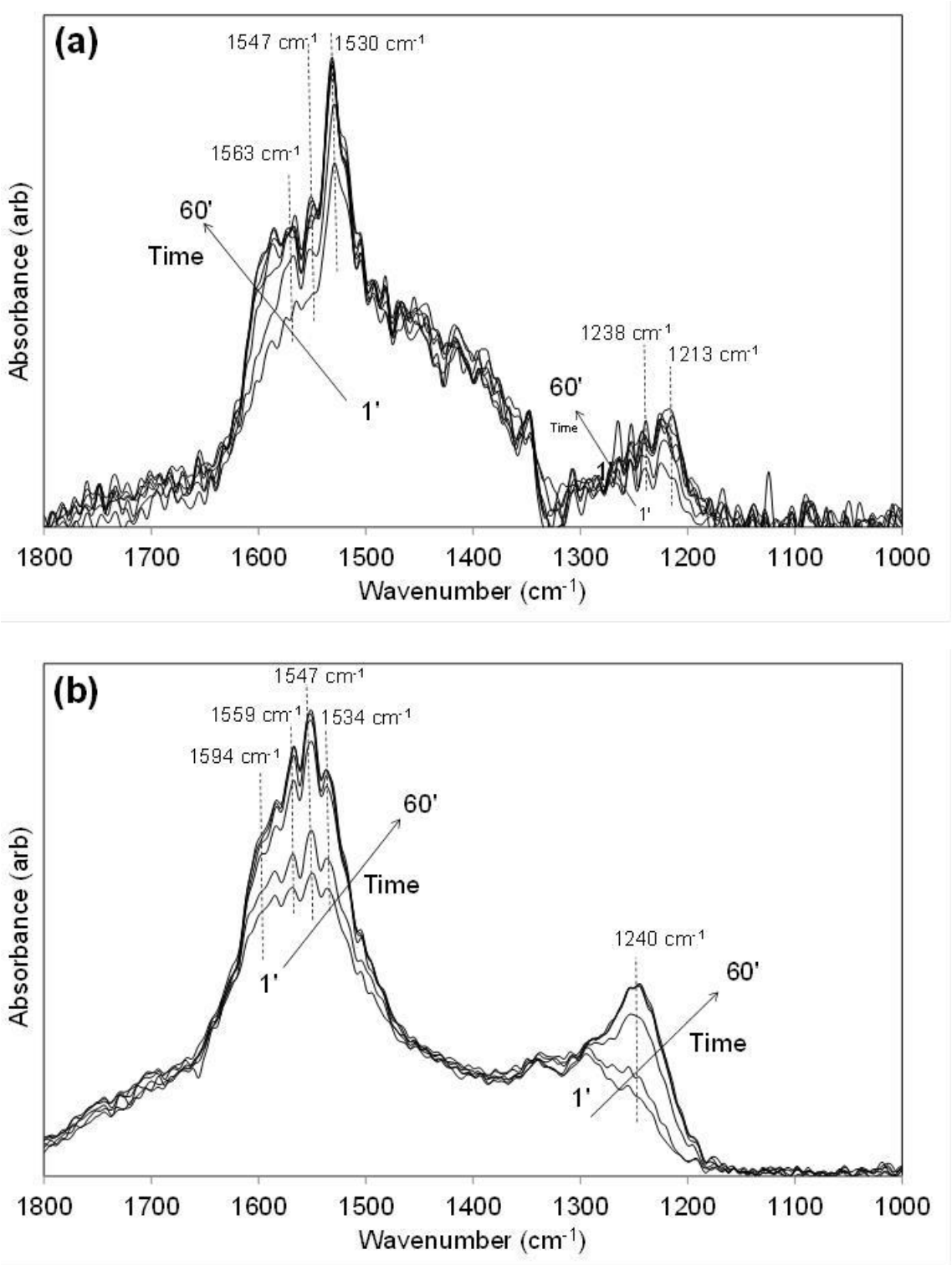

Figure 7. DRIFT spectra obtained in a $NOx/O_2/CO_2/N_2$ atmosphere with (a) $Ce_{0.73}Zr_{0.27}O_2$ and (b) $Ce_{0.64}Zr_{0.27}Nd_{0.09}O_2$.

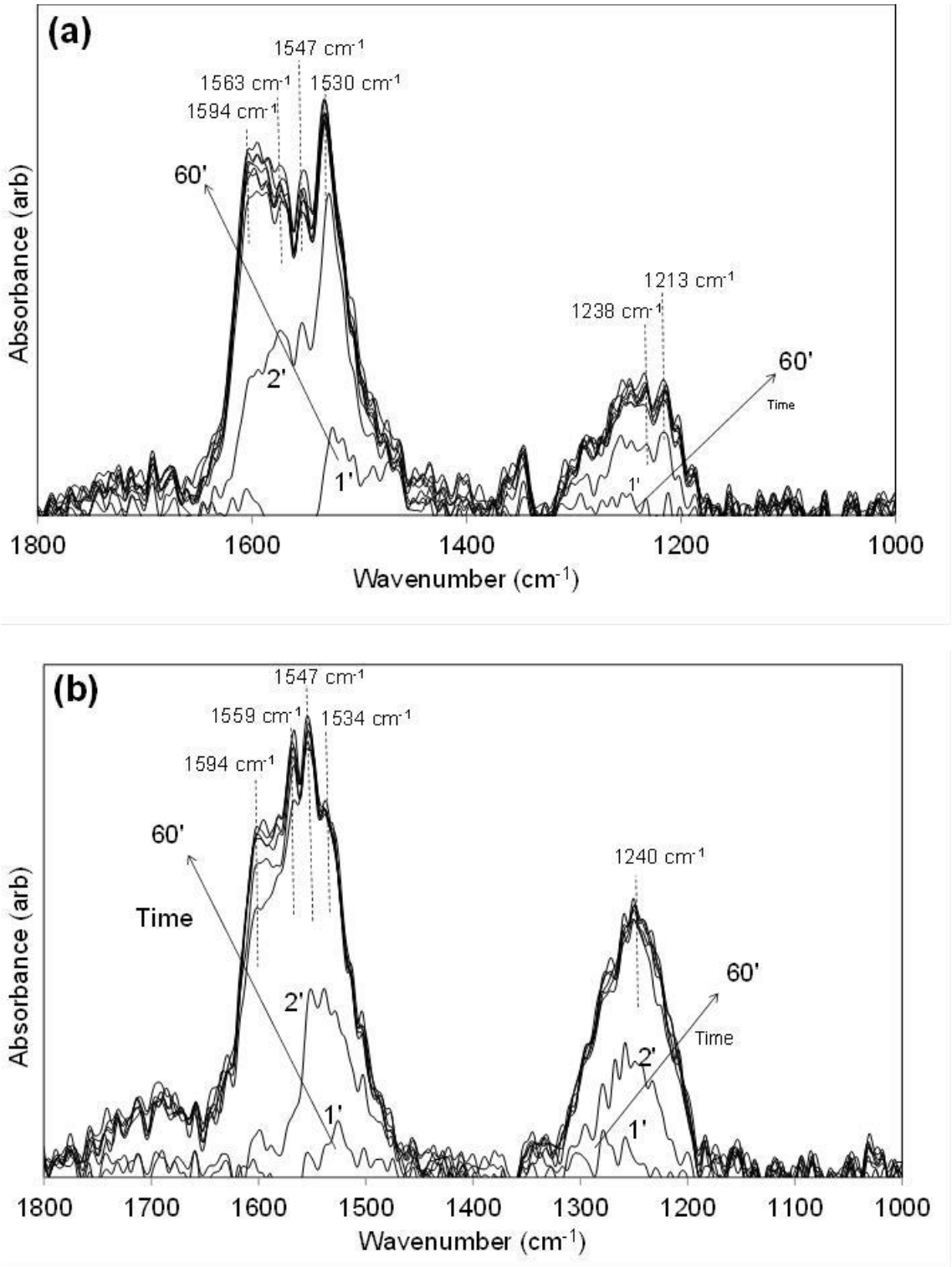

Figure 8. DRIFT spectra obtained in a $NOx/O_2/H_2O/N_2$ atmosphere with (a) $Ce_{0.73}Zr_{0.27}O_2$ and (b) $Ce_{0.64}Zr_{0.27}Nd_{0.09}O_2$.

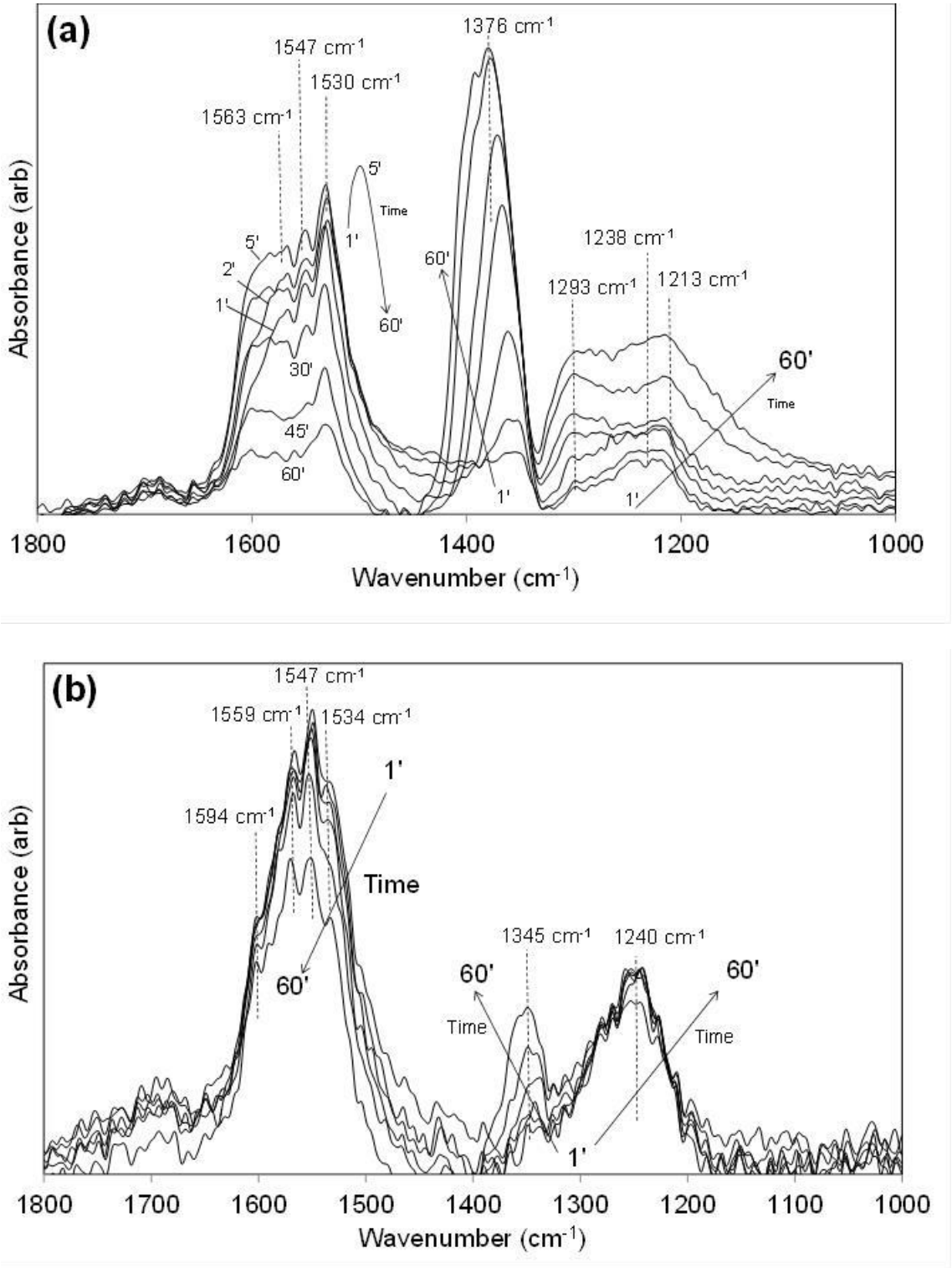

Figure 9. DRIFT spectra obtained in a $NOx/O_2/SO_2/N_2$ atmosphere with (a) $Ce_{0.73}Zr_{0.27}O_2$ and (b) $Ce_{0.64}Zr_{0.27}Nd_{0.09}O_2$.